Plasma Science and Technology

PAPER

Occurrence of ionization instability associated with plasma bubble in glow discharge magnetized plasma

To cite this article: Mariammal MEGALINGAM and Bornali SARMA 2019 *Plasma Sci. Technol.* **21** 115402

Plasma Sci. Technol. **21** (2019) 115402 (9pp) https://doi.org/10.1088/2058-6272/ab2ef2

Occurrence of ionization instability associated with plasma bubble in glow discharge magnetized plasma

Mariammal MEGALINGAM and Bornali SARMA

Division of Physics, Vellore Institute of Technology, Vandalur-Kelambakkam Road, Chennai 600127, Tamilnadu, India

E-mail: bornali_s2000@yahoo.co.in

Received 2 May 2019, revised 29 June 2019
Accepted for publication 3 July 2019
Published 23 August 2019

Abstract

Floating potential fluctuations of glow discharge magnetized plasma are found to expose mixed mode oscillations (MMOs) in the existence of plasma bubble. Plasma bubble has been formed by emerging density gradient in the form of a sheath around a cylindrical and spherical grid to a critical value of applied potential. Two Langmuir probes, LP_1 and LP_2, are retained in the ambient plasma to collect the plasma floating potential fluctuations at two different locations of the plasma system. The perceived instability pattern shows regular-irregular-regular MMOs under various imposed conditions. Furthermore, various nonlinear techniques such as phase space plot, recurrence plot and Hurst exponent have been executed to understand the underlying dynamical behavior of the system. Low-frequency (∼200–1200 Hz) oscillations are also supposed and are inferred as ion-acoustic waves excited by ionization instability. The observed results are then validated with the theory of the instability based on a fluid hydrodynamic approach.

Keywords: plasma bubble, floating potential fluctuations, MMO, instability

(Some figures may appear in colour only in the online journal)

1. Introduction

The sheath phenomenon in plasmas is a broad topic of interest ranging from laboratory to space plasmas. A sheath arises at the interfaces between plasma and a solid or electrode, which serves to control fluxes of electrons and ions. Initially, a plasma sheath was originated for plane geometries [1] and later on expanded to various geometries such as cylindrical [2] and spherical [3]. The importance of introducing a grid is of great interest for ion beam sources [4], velocity analyzers [5], electrostatic confinement schemes [6] and antennas for electrostatic waves. In a double plasma device, low-frequency waves are impulsively excited in a double layer generated by ion injection into the target chamber [7]. Stenzel *et al* [8, 9] have reported several experimental studies on plasma bubble by introducing a spherical mesh grid in ambient plasma. Double sheath study has been done by biasing the mesh grid negatively and is termed plasma 'bubble'. Glow discharge plasma is the best stage to study and comprehend various nonlinear phenomena such as a complex, chaotic dynamical system, etc. Since various dynamical processes take place in the plasma, it becomes favorable to the excitation of waves and instabilities [10].

The source of the instability arises when the system is perturbed by a controlling parameter where various nonlinear phenomena viz. quasi-periodic, period doubling, mixed mode oscillations (MMOs), canard oscillations, etc, can be observed experimentally in many physical, chemical, biological systems, etc [11]. Nevertheless, only a few plasma experiments have exposed such kinds of phenomena. Moreover, most of the nonlinearity relies on the excitability of plasma, which can perform in the glow discharge plasmas. We could observe the nonlinear phenomena such as stochastic resonance, coherence resonance, period doubling, order to chaos oscillations [12], irregular to regular mode oscillations [13] and other perturbation-boosted nonlinear phenomena [14, 15] whenever the

plasma is disturbed in its excitable state using any control parameter, noise or a periodic signal. It is understood that if the system is perturbed using noise, discharge voltages, external magnetic field, etc, it shows MMO. The oscillation occurs when a dynamical system shifts from fast to slow motion and vice versa and hence, the small and large amplitude can be called an MMO [16]. MMOs can execute in several systems in nature and may be simple or complex. MMOs of this type are omnipresent in nature; during the 1970s, experimentation first took place with Belouzov–Zhabotinsky (BZ) chemical reactions. MMOs are also initiated in chemistry on surface chemical reactions, in medicine on neural systems, electro cardiac dynamics, etc. Mikikian *et al* [17] reported the study and existence of MMOs in dusty plasmas in the beginning. The evolution of interspike interval and its frequencies has been explored. Observation of MMOs in glow discharge has been reported [18] and there are two kinds of oscillations, i.e. small quasi-periodic oscillations and MMOs in the presence and absence of a magnetic field. The formation of MMO in a system has been explained by Hudson *et al* [19] in BZ reaction in a well-stirred flow reactor. Multi-peaked states denoted as MMO and their appearance are of two distinct modes of oscillation: small-amplitude nearly harmonic oscillations and large-amplitude relaxation oscillations. An occurrence of MMOs is based on slow manifold models. When a system is characterized by time scales, which differ by several orders of magnitude, the system will devote most of the time on a surface in phase space on which the motion is relatively slow. When the system is disturbed away from the surface, it will in contrast relax very fast. MMOs ascend when the dynamics on the slow manifold is oscillatory and there is no attractor within the slow manifold. However, well-known techniques for the nonlinear time series analysis such as power spectrum and Lyapunov exponent [20] can extract only global and asymptotic properties of the system and they are idle for separating local structures.

Generally, exciting phenomena such as intermittency or MMOs can arise from the nonlinear interaction of different kinds of ionization waves. In this work, an attempt has been made to study the characteristics of observed MMOs and their induced ionization instability in glow discharge magnetized plasma. Plasma floating potential fluctuations (FPFs) are collected at two different positions and it is found that it shows a transition from regular to irregular to regular MMOs with increasing discharge voltage (V_d) keeping the magnetic field fixed. As the discharge voltage gradually increases, initially regular MMOs are noted. Further increasing V_d, the FPF grows as regular to irregular to regular MMO. A qualitative understanding has been gained from the power spectrum, phase space plot (PSP) and recurrence plot (RP). The PSP reveals that the fluctuations have large and small loops with respect to the discharge voltage. Visual changes in the RP are the noble method to detect the transition in FPF. But, for quantitative knowledge, we have carried out Hurst exponent analysis, which explains the system has different types of oscillations. From fast Fourier transform, we have also found that the existing frequencies are low and are comparable with ionization wave frequencies. However, the observed low-range frequency sustains the properties of ion-acoustic waves. Such waves are excited by ionization instability. In order to understand the excited wave and its growth rate, numerical modeling has been done and it has been found that ion viscosity is responsible for creating such low-frequency ionization instability.

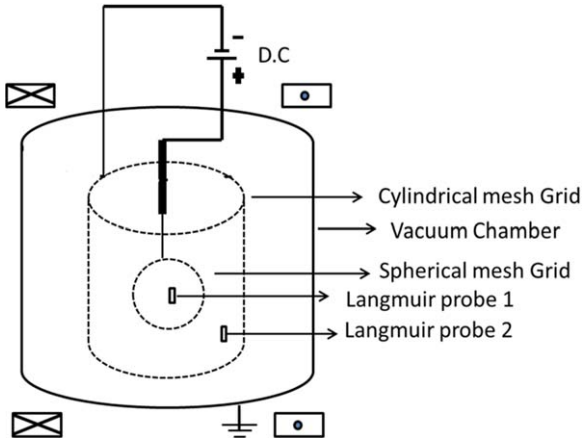

Figure 1. Schematic diagram of the experimental setup.

The layout of this work is as follows. Section 2 shows the experimental setup. In section 3, experimental results are presented followed by analysis and discussion. Section 4 contains the numerical modeling and section 5 gives the conclusion of the work.

2. Experimental setup

Figure 1 demonstrates the plasma chamber in which we have a cylindrical stainless-steel chamber 50 cm in length and 40 cm in diameter. Two mesh grids of different shapes, viz. a cylindrical one 20 cm in height and 15 cm in diameter and a spherical one 15 cm diameter with 80% optical transparency are located in the middle of the chamber. The cylindrical mesh grid is the cathode and the spherical mesh grid is the anode, which is connected to the constricted electrode. Once the chamber is evacuated to a base pressure of 9.2×10^{-3} mbar, it is occupied by Ar gas to a pressure of 2.3×10^{-1} mbar. Plasma is created by a DC power supply, which can be changed from 0 to 1000 V. But for this particular study, it is operated in the range of 240–280 V. The magnetic field is produced using Helmholtz coil looped around the plasma chamber. The diagnostic tool, viz. a Langmuir probe of 2.0 mm diameter is used to measure the plasma FPFs. The plasma density and electron temperature are found to be of the order of 10^8 cm^{-3} and 1−3 eV. Two Langmuir probes, viz. LP_1 and LP_2 are retained in different fixed positions to examine the dynamical transition of the FPFs inside the spherical mesh grid and in between the cylindrical and spherical mesh grid. The signals picked up by the Langmuir probes are acquired by the FPF data directly in the oscilloscope with a bandwidth up to 400 MHz and storage up to 2.58×10^6 samples.

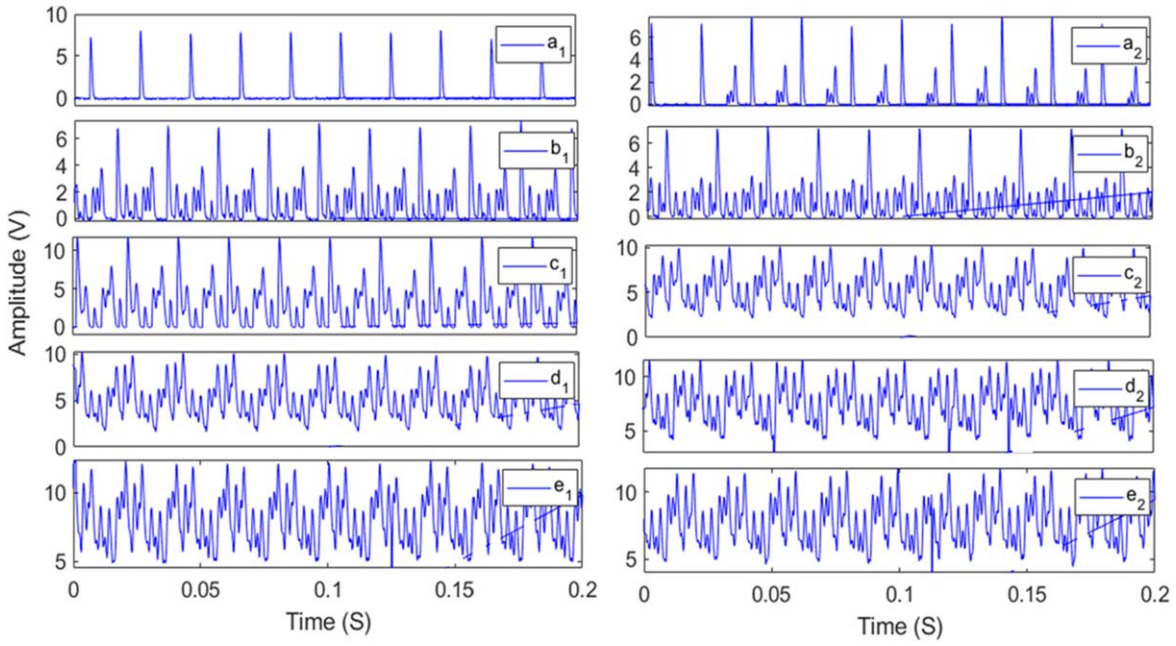

Figure 2. FPF for various V_d. (a) 240 V, (b) 250 V, (c) 260 V, (d) 270 V, (e) 280 V by the inner (a_1)–(e_1) and the outer Langmuir probes (a_2)–(e_2) at $B = 52$ G.

3. Experimental results and analysis

The experiment that has been carried out in the argon gas shows interesting features for increasing the discharge voltages (V_d) from 240 to 280 V at 52 G magnetic field and V_d has been taken as a controlling parameter. The dynamics of the oscillations is delicate to the controlling parameter and with the variation of such parameters. Thus, it illustrates regular to irregular to regular MMOs. The observed MMOs could be attributed to a situation where the ionization instability occurs. As the discharge voltage increases, the system is favorable for the growth of ion-acoustic instabilities [21]. This is because when the discharge is formed initially, single mode with small peaks is observed, as V_d increases the number of modes in the oscillations. The MMO pattern characterized by large (L) and small-amplitude (s) oscillations is denoted by L^s. Accordingly, it is observed that the pattern takes the form of $1^6 1^1 1^1$. This is attributed to the ionization instabilities. This signifies that there is an increase in the density and therefore there is an ion-acoustic turbulence related to ionization instabilities.

The plasma FPFs have been measured at two different positions in between the spherical and cylindrical mesh grid (LP_1) and near the chamber wall (LP_2), which exhibit the behavior of MMOs. In this study, discharge voltage is taken as a control parameter with fixed magnetic field 52 G. Figures 2(a_1)–(e_1) show the observed time series by LP_1, i.e. in between the spherical and cylindrical grid. At low discharge voltage $V_d = 240$ V, a single period of oscillations with much lower amplitude fluctuations are initiated with clearly separable amplitudes, as shown in figure 2(a_1). The large and small oscillations do not follow any sequential recurrence at 250 V. Hence, they can be considered as irregular MMOs, since the periodicity is lacking. The scenario of FPF at 250 V has the oscillation block-like $1^5 1^1$ along with oscillation $1^5 1^0$ and so on. The FPF at 260 V is also an irregular MMO and its oscillation blocks are initiated with the pattern $1^4 1^1$ then $1^5 1^1$ in a random manner. Further increasing the discharge voltage to 270 V, an order blocks as $1^6 1^1 1^1$ and its recurrences can be understood in the entire time series, as shown in figure 2(d_1), which transform into regular MMOs from irregular MMOs. At around $V_d = 280$ V, again a regular MMO has been observed in the pattern $1^1 1^7 1^1$ throughout the time series, as illustrated in figure 2(e_1). Therefore, the observed MMOs occur in single period—irregular–regular mode, as V_d is enhanced [22]. Figures 2(a_2)–(e_2) show the observed time series by LP_2, i.e. near the chamber wall. For $V_d = 240$ V, 1^3 blocks of oscillations occurred and further increasing V_d, reduced it to 1^2 blocks though continuing a regular pattern. At around 260 V, the observed pattern is $1^1 1^3 1^5$ and for the higher V_d, the MMO structure is $1^2 1^1 1^3$. Therefore, it can be inferred that as the discharge voltage increases, the dynamics of the system shows a variety of MMOs. This is attributed to the fact that because of ionization, such a kind of dynamics has been observed. It is also suggested that as V_d is increased, the rate of ionization also increases leading to a greater number of charged particles and hence the observed oscillations may be termed ionization instability.

The power spectrum of the FPFs has been explored to gain an understanding of the nature of the dynamics of the system. Figure 3 shows the power spectrum of FPF obtained by LP_1 and LP_2 where we can gather the information of existing frequency components, which contribute to the resultant MMO. Figure 3(a_1) shows a clear picture of more distinct peaks for $V_d = 260$ V. On further increasing $V_d = 250$ V, the dominant frequency of 604 Hz has been observed with high amplitude, which reflects that the

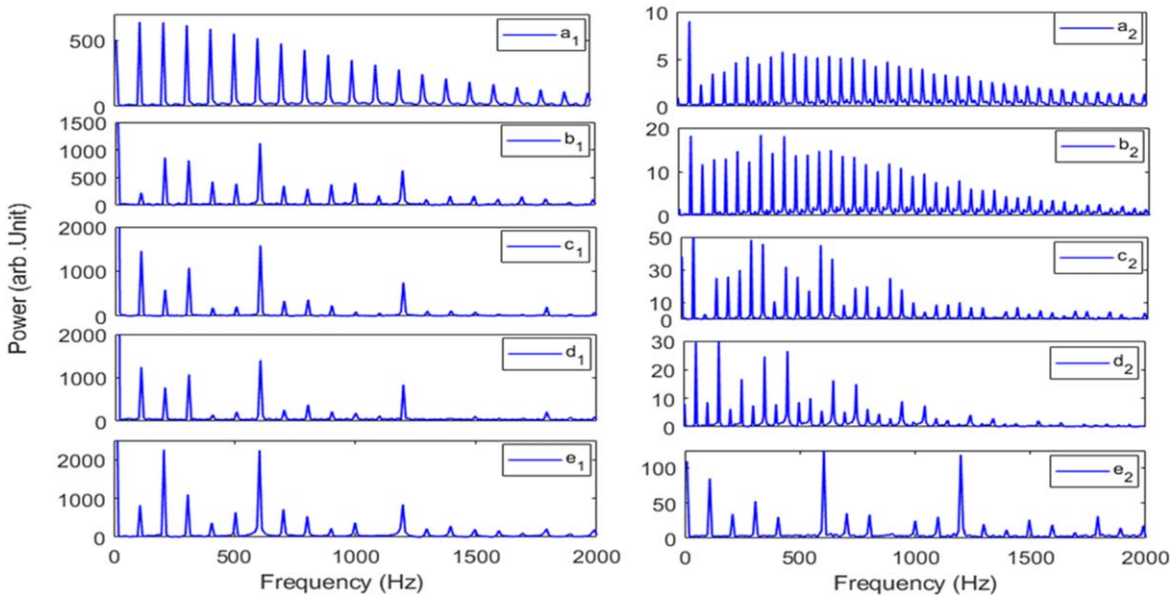

Figure 3. Power spectra for various V_d. (a) 240 V, (b) 250 V, (c) 260 V, (d) 270 V, (e) 280 V by the inner (a_1)–(e_1) and the outer Langmuir probes (a_2)–(e_2) at $B = 52$ G.

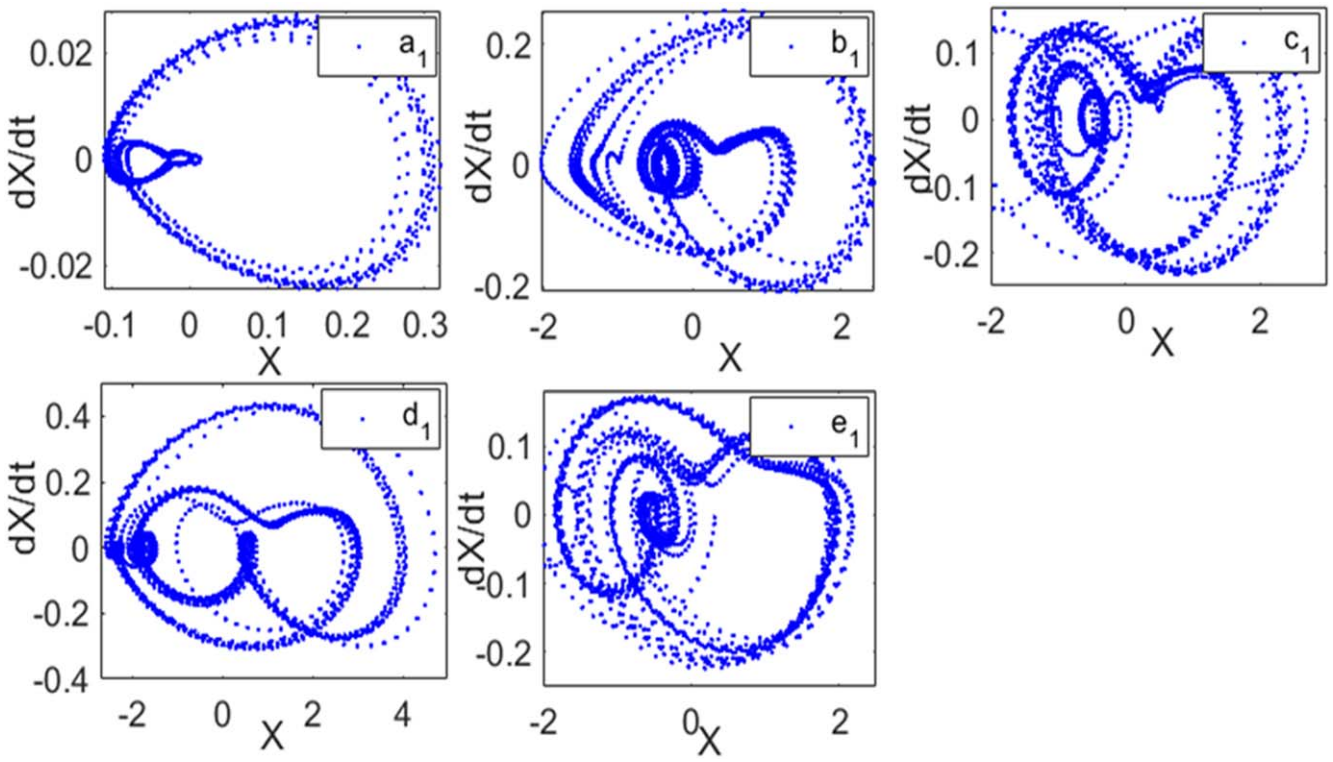

Figure 4. PSP of FPFs by the inner Langmuir probe LP_1 at $B = 52$ G for different discharge voltages: (a_1) 240 V, (b_1) 250 V, (c_1) 260 V, (d_1) 270 V, (e_1) 280 V.

ionization plays a significant role. At about 270 V discharge voltage, more peaks are present reflecting the nature of MMO; these are 306 and 604 Hz, as shown in figure 3(d_1). At the highest discharge voltage $V_d = 280$ V, the dominant frequencies are 207.9 and 604 Hz with greater amplitudes. Likewise, figure 3(a_2) shows a greater number of clear distinct peaks, which explains the nature of MMO at $V_d = 240$ V. Further increasing V_d to 250 and 260 V, more peaks arose with lower amplitude compared to LP_1 fluctuations. For the higher V_d, it has been observed that the dominant frequencies are 604 and 1198 Hz, as illustrated in figure 3(e_2). The frequencies seen in the power spectra are low frequency and can probably be compared with ionization wave frequencies.

In complex dynamics such as MMO, one can expect a greater number of points of attraction in which the phase space trajectory evolves. Here, the PSP has been done

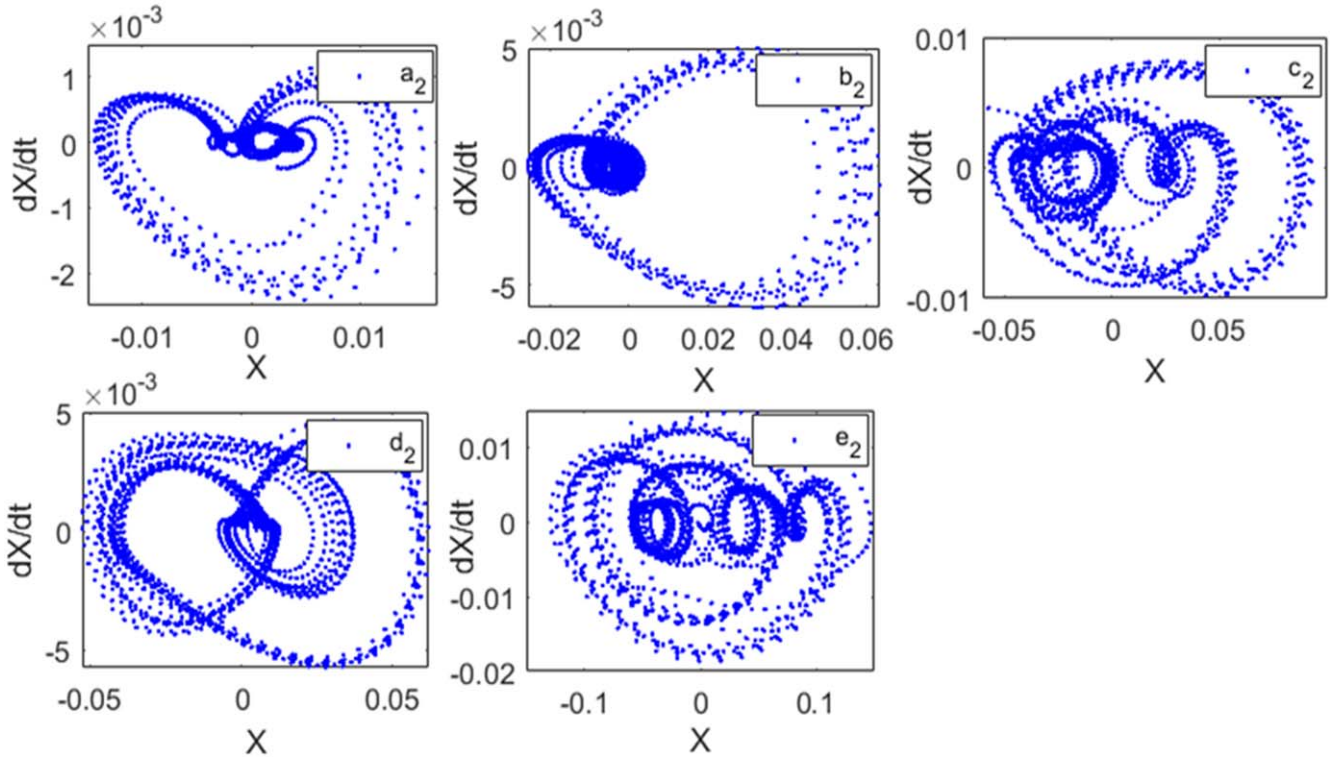

Figure 5. PSP of FPFs by the outer Langmuir probe LP_2 at $B = 52$ G for different discharge voltages: (a_2) 240 V, (b_2) 250 V, (c_2) 260 V, (d_2) 270 V, (e_2) 280 V.

through the time series using a time-delay method. In this particular experiment, the PSP has closed paths and it can be divided into two groups, i.e. large oscillations corresponding to big loops and the interlaced small oscillations corresponding to the small loops. At the lower discharge voltage $V_d = 240$ V, periodic MMOs have been observed with small and large loops, as shown in figure 4(a_1). When it comes to irregular MMO, data points are spread out of the path in (outer loops) a random manner, as shown in figure 4(b_1). The same scenario is continued with $V_d = 260$ V and with further increasing voltages, regular MMOs appearing on the reconstructed path are clearer, as demonstrated in figure 4(e_1).

Similarly, we have observed the nature of MMO measured by LP_2 from figures 5(a_2)–(e_2) for different discharge voltages. Therefore, figures 4(a_1)–(e_1) reflect the nature irregular to regular MMO, whereas figures 5(a_2)–(e_2) explain the nature of the loops with respect to varying discharge voltages.

Figures 6 and 7 show the RPs of FPF at 52 G magnetic field and different discharge voltages. A large diagonal line with small dots reveals the presence of large and small oscillations, as shown in figure 6(a). This can be compared with the time series signal in figure 2(a_1). As the discharge voltage increases, the occurrence of new modes in the fluctuations is observed in figure 6(b) and it is noted as $1^5 1^0$ and $1^5 1^1$ in time series signals. When at slightly higher $V_d = 260$ V, dark spots on the diagonal lines are observed reflecting that the number of blocks in the oscillations increased, which is in the recurrence of $1^4 1^1$ and $1^5 1^1$. The distance between the diagonal lines is studied under the variation of V_d, which infers the frequency of oscillation that alters with different discharge voltages. On further increasing to 270 V, dark spots are overlapped with the diagonal lines along with small dots, which explains the nature of the fluctuations as $1^6 1^1 1^1$. For the higher discharge voltages, noninterrupting diagonal lines with dark spots can be seen in figure 6(e). This explains the existence of the new blocks of oscillations in the pattern $1^1 1^7 1^1$.

Figure 7 shows the pictorial representation of MMOs. When the discharge voltage is 240 V, strong diagonal lines and dotted lines can be observed in figure 7(a), which reflect the periodic nature of the fluctuations. As V_d increases to 250 V, a greater number of periodic lines is observed with dark dots reflecting $1^2 1^2 1^2$, as shown in figure 7(b). A similar pattern has been observed for other V_d also and for higher $V_d = 280$ V, long diagonal lines along with dots, which explain the occurrence of new modes in the nature of the fluctuations as $1^2 1^1 1^3$.

Moreover, the progression of nonlinearity of the dynamical system with respect to the controlling parameter can be known by reviewing some of the system properties. Here, in this study, we have carried out a Hurst exponent in order to know the periodicity and persistence of the time series. In general, the characteristics of the system can be known by analyzing the order at which the oscillations of a time series appears. The Hurst exponent is said to be chaotic if there is no recurrence in the sequence [23]. If the sequence follows a trend, it is persistent with $0.5 < H < 1.0$. At the same time, if the sequences of the trend change rapidly or very often, then it is an anti-persistent behavior with Hurst exponent values of 0.5. Figure 8 shows the Hurst exponent along with its discharge voltages for LP_1 and LP_2. The regular MMOs have been observed for the lower discharge voltage 240 V by LP_1,

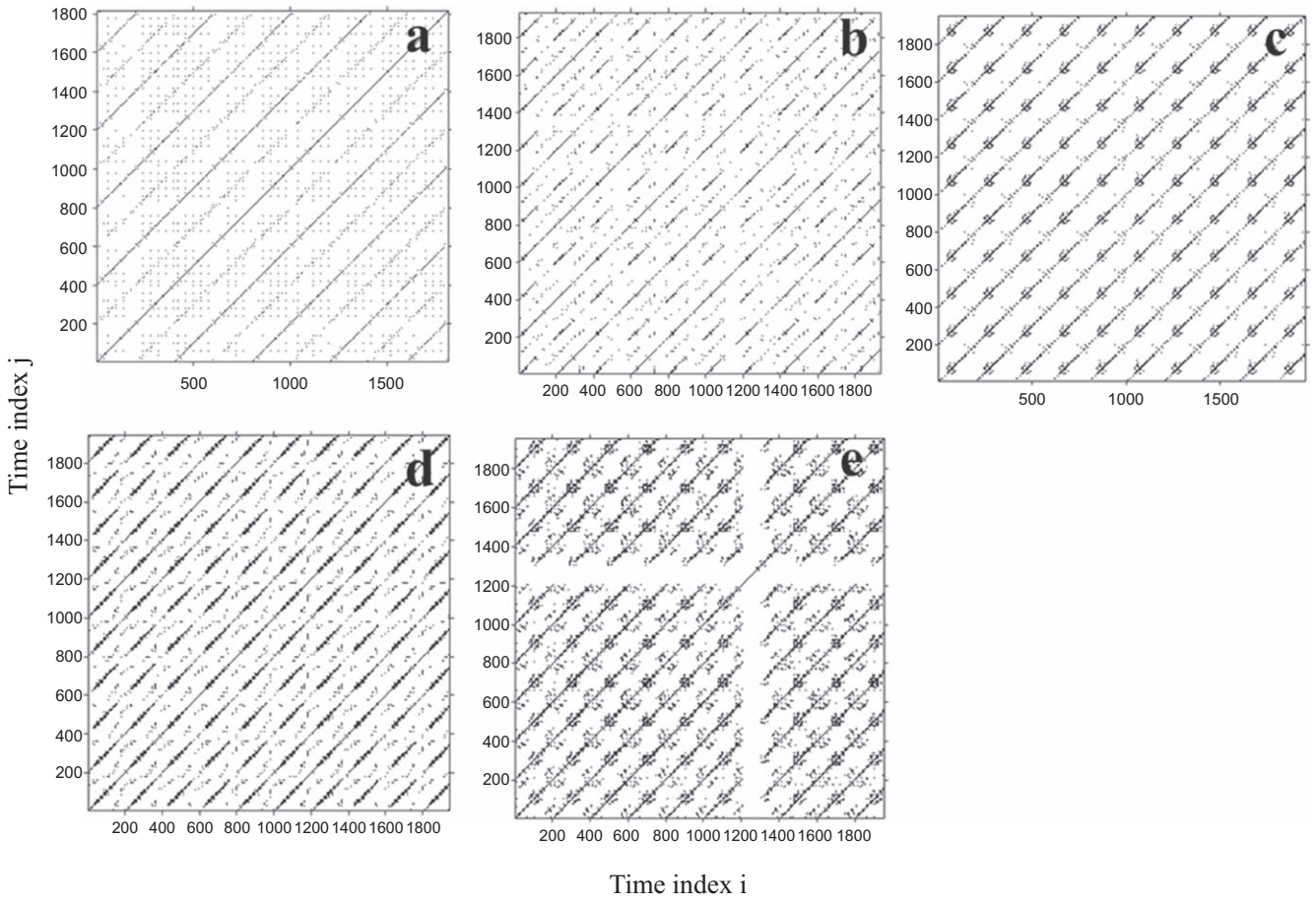

Figure 6. RP of FPFs by the outer Langmuir probe LP_1 at $B = 52$ G for different discharge voltages: (a) 240 V, (b) 250 V, (c) 260 V, (d) 270 V, (e) 280 V.

which exhibit a value of Hurst exponent 0.7413. As the V_d increases to 250 V, the exponent increases to 1.0045 where irregular MMOs have been observed. Therefore, it can be considered as persistent oscillation. With further increment of V_d to 260 V, irregular MMOs can still be seen and there is a fall in the exponent (0.9070) at around 270 V as long as regular MMOs are seen in the time series. Similarly, for LP_2, we can see the increasing trend of the Hurst exponent. At lower discharge voltages, the Hurst exponent is 0.8602 and only a further growing trend of H has been observed till the higher discharge voltages. Therefore, it can be concluded that there are two types of oscillations existing in the system.

4. Ionization instability

This section explains how ion-acoustic waves could be excited in plasma in a low degree of ionization, where energetic electrons are present to ionize the neutral gas. In DC glow discharge magnetized plasma, we have observed a variety of MMOs for increasing discharge voltages. It is speculated that the observed instability may be due to the ionization mechanism. It is understood from the literature [24] that if the wave should be the ion-acoustic wave, then it should have a broad feature of low frequency. The ion-acoustic waves can be excited only at relatively high pressure. Therefore, in our study, we have taken 2.3×10^{-1} mbar as a working pressure and also found the existing frequencies ranging from 200–1200 Hz and the peak amplitude is around 10 V. For the higher discharge voltage at 280 V, the dominant frequency has been observed as 600 Hz and the axial wavelength under this condition appears to be $\lambda \approx 50$ cm. Hence, the phase velocity ν has been calculated as $\sim 3 \times 10^4$ cm s^{-1} for this particular experiment.

The way in which ionization can produce growth of ion-acoustic waves can be easily visualized and understood. If an ion-acoustic disturbance of very slight amplitude exists in the plasma, then the regions equivalent to the wave's crest are moreover the regions of higher potential, i.e. higher plasma density [25]. If we suppose the ionizing electrons have greater energy than the ionization threshold, then the ionization cross-section is a quickly growing function of the electron energy over an electron interval of range 20–30 eV. Consequently, ionization of the neutral gas will continue at a rate larger in the wave troughs than in the wave crests. Thus, the waves might grow if the damping mechanisms are present and are not too strong [26]. To know the growth mechanism of plasma waves, we have assumed ions and electrons as fluids. Considering Boltzmann equilibrium for electrons $kT_e \nabla n = en \nabla \varphi$ where T_e

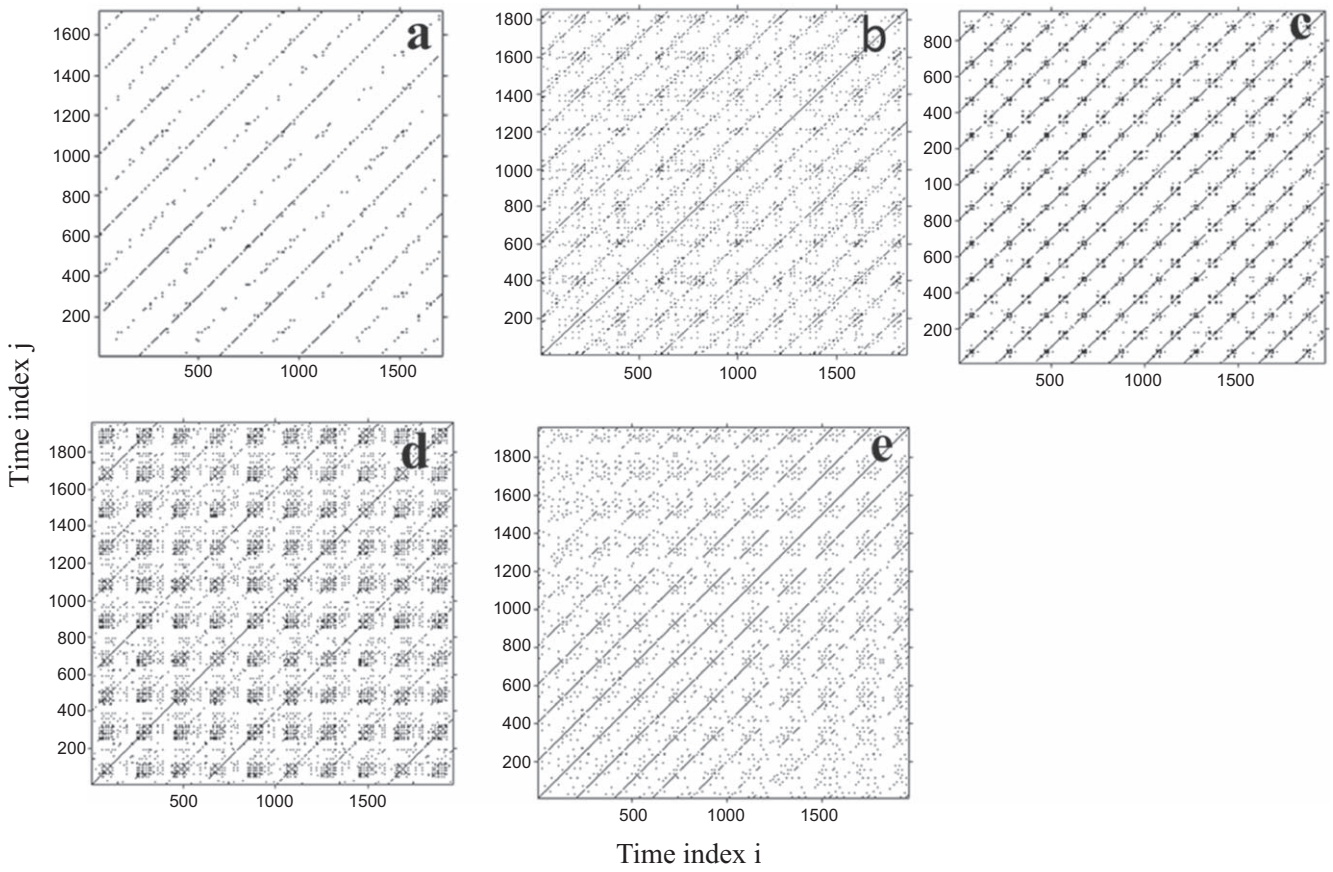

Figure 7. RP of FPFs by the outer Langmuir probe LP_2 at $B = 52$ G for different discharge voltages: (a) 240 V, (b) 250 V, (c) 260 V, (d) 270 V, (e) 280 V.

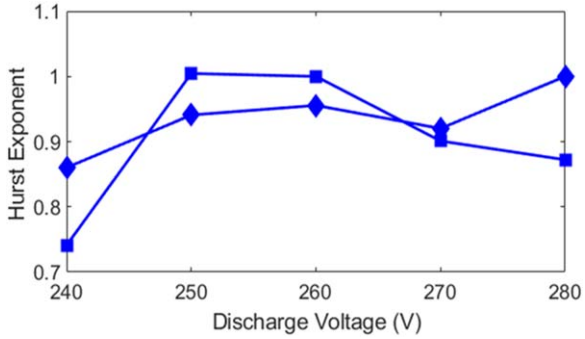

Figure 8. Plot of Hurst exponent versus different discharge voltages for constant B.

is the temperature of the electron, n is the plasma density, φ is the electric potential, k is the Boltzmann constant and e is the electron charge.

Considering the conditions $T_i \ll T_e$ and taking the ion continuity and momentum equations in 1D as

$$\frac{\partial n}{\partial t} + \frac{\partial}{\partial z}(n\nu) + \frac{n}{\tau_L} - Q = 0, \tag{1}$$

$$nm\frac{\partial \upsilon}{\partial t} + nm\upsilon\frac{\partial \upsilon}{\partial z} + en\frac{\partial \varphi}{\partial z} + \nu nm\upsilon - nm\beta\nabla^2\upsilon + Qm\upsilon = 0, \tag{2}$$

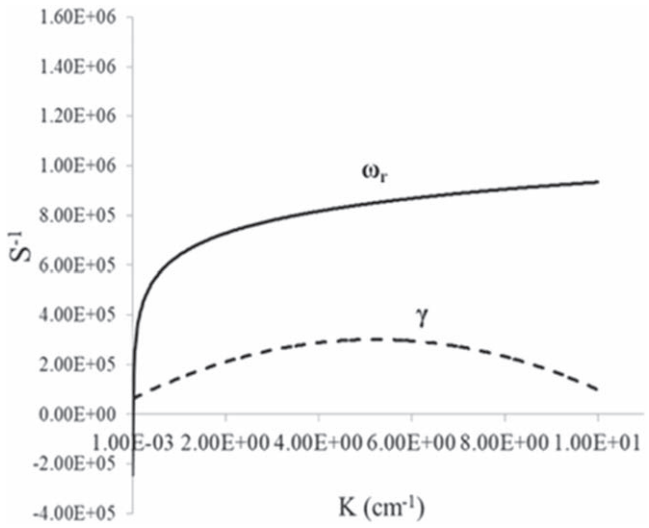

Figure 9. Representation of ionization instability (Wave angular frequency and its growth rate with respect to the wave number K).

where $\frac{n}{\tau_L}$ from equation (1) represents the ion losses, which may be present with loss time τ_L and Q denotes the production rate of new ions generated by the ionization process.

Therefore, Q can be written as

$$Q = \sigma_1 N \varnothing, \tag{3}$$

where σ_1 is the cross-section of ionization, N signifies the gas density of neutral particles and $\varnothing$ is the ionizing electron flux. From equation (2), the term νnmv signifies momentum losses by an ion when it is colliding with neutral gas with the collision frequency ν. The term Qmv from equation (2) represents the production of new ions whose average velocity is different to the instantaneous velocity of the ion fluid [23]. The term $-nm\beta\nabla^2 v$ denotes the effect of viscosity where β is the kinematic viscosity coefficient.

Linearization of equations (1) and (2) has been done by the ordinary method and the space and time variation of the first-order quantities has been taken to be of the type $\exp \mathrm{i}(Kz - \omega t)$, and here K is the wave number and ω is the angular frequency.

Thus, the dispersion relation can be of the form

$$\omega^2 + \mathrm{i}\left[\nu + \beta K^2 + \frac{2}{\tau_\mathrm{L}} - \left(\frac{\mathrm{d}\sigma}{\mathrm{d}\varphi}\right)_0 \frac{N\varnothing}{n_0}\frac{kT_\mathrm{e}}{e}\right]\omega - \left[\frac{1}{\tau_\mathrm{L}} - \left(\frac{\mathrm{d}\sigma}{\mathrm{d}\varphi}\right)_0 \frac{N\varnothing}{n_0}\frac{kT_\mathrm{e}}{e}\right]\left(\nu + \beta K^2 + \frac{1}{\tau_\mathrm{L}}\right) - K^2 C_\mathrm{s}^2 = 0, \tag{4}$$

where $C_\mathrm{s} = \left(\frac{kT_\mathrm{e}}{m}\right)^{1/2}$ represents the ion-acoustic speed. Considering K to be the wave number and to be real, and ω the frequency to be complex with $\omega = \omega_\mathrm{r} + \mathrm{i}\gamma$. The positive value of the growth rate γ resembles the wave growth, whereas a negative value γ the wave damping.

Thus, the dispersion relation (4) can be detached into real and imaginary parts and it can be written as

$$\omega_\mathrm{r}^2 = K^2 C_\mathrm{s}^2 - \left(\gamma + \nu + \beta K^2 + \frac{1}{\tau_\mathrm{L}}\right)^2, \tag{5}$$

$$\gamma = \frac{1}{2}\left[\frac{1}{\tau_\mathrm{L}}\left(\frac{\Delta\sigma}{\sigma_0} - 1\right) - \left(\nu + \beta K^2 + \frac{1}{\tau_\mathrm{L}}\right)\right], \tag{6}$$

where $\Delta\sigma = \left[\left(\frac{\mathrm{d}\sigma}{\mathrm{d}(e\varphi)}\right)_0 kT_\mathrm{e}\right]$.

It is understood from equation (5) that the growth rate in positive value can be attained only when the ionization cross-section with the electron energy is adequate to control the damping effects of collisions between the particles, viscosity and loss of ions. However, the waves can be comparable with ion-acoustic waves, which reflects that ω_r is growing exponentially with respect to the K value due to ion viscosity. However, the positive growth rate γ is maintained fairly well for the particular range of K values shown in figure 9.

Therefore, it can be concluded that ion viscosity plays a role and is the background reason for the occurrence of low frequency in the observable waves. Furthermore, this also explains that the waves can be excited if there is no boundary in the uniform plasma and also in the low-frequency range. Hence, one would also suppose that frequency may start from low (200 Hz) to the upper limit (1200 Hz) by the ion viscosity. It would appear that whatever the nonlinearity present in the system and its dimensions, it is liable for directing the oscillation energy into growth of the ionization instability.

5. Conclusion

A variety of MMOs have been studied in glow discharge plasma by increasing V_d, wherein initial regular MMO was observed. With the further increase of V_d, the fluctuation trend shows a transition from regular to irregular to regular MMOs. The power spectrum reveals that for the higher discharge voltage, the observed dominant frequencies are 604 and 1198 Hz. It has also been noted that these are low frequencies and they are comparable with ionization wave frequencies. In addition, observation from PSP explains that the FPF consists of large loops along small loops reflecting the nature of MMO. The RP is one of the powerful tools for the visualization and analysis of dynamical systems, which also reveals the similar transition pattern of the system. The RP shows extensive variation in the diagonal lines in the pattern, which enumerates that as V_d increases, the number of modes in the fluctuations also increases in a respective manner. Therefore, the observed low-frequency oscillations satisfy the properties of ion-acoustic waves; such waves are excited by ionization instability. We have also carried out a numerical modeling in order to study the excited wave frequency along with its growth rate. It has been observed that ω_r grows exponentially with respect to the K value due to ion viscosity. However, the positive growth rate γ is also maintained fairly well for the particular range of K values. It is also understood that the ion viscosity is one of the prime factors responsible for low-frequency ionization instability.

Acknowledgments

The authors would like to thank ISRO, Government of India, for providing financial support for the research work (Grant No. ISRO/RES/2/391/2014-15).

References

[1] Mott-Smith H M and Langmuir I 1926 *Phys. Rev.* **28** 727
[2] Laframboise J and Rubinstein J 1976 *Phys. Fluids.* **19** 1900
[3] Allen J E 1999 *Phys. Scr.* **45** 497
[4] Salvadori M C *et al* 2011 *J. Appl. Phys.* **110** 083308
[5] Donoso G and Martin P 1986 *Rev. Sci. Instrum.* **57** 1501
[6] Dolan T J *et al* 1972 *J. Appl. Phys.* **43** 590
[7] Johnson J C, Angelo N D and Merlino R L 1990 *J. Phys.* D **23** 682
[8] Stenzel R L and Urrutia J M 2012 *Phys. Plasmas* **19** 082105
[9] Stenzel R L and Urrutia J M II 2012 *Phys. Plasmas* **19** 082106
[10] Marino F *et al* 2004 *Phys. Rev. Lett.* **92** 073901
[11] Lin I and Liu J M 1995 *Phys. Rev. Lett.* **74** 3161
[12] Megalingam M *et al* 2016 *Phys. Plasmas* **23** 072102
[13] Megalingam M *et al* 2017 *Phys. Plasmas* **24** 042304
[14] Kumar R, Narayanan R and Prasad A 2014 *Phys. Plasmas* **21** 123501
[15] Saha D *et al* 2014 *Phys. Rev.* **28** 032301
[16] Brons M *et al* 2008 *Chaos* **18** 015101
[17] Mikikian M 2008 *Pure Appl. Chem.* **100** 225005
[18] Shaw P K, Iyengar A N S and Nurujjaman M 2015 *Phys. Plasmas* **28** 122301

[19] Hudson L, Hart M and Marinko D 1979 *J. Chem. Phys.* **171** 1601
[20] Feder J 1988 *Fractals* (New York: Plenum)
[21] Lahiri S, Roychowdhury D and Sekar Iyengar A N 2012 *Phys. Plasmas* **19** 08231
[22] Ghosh S *et al* 2015 *Phys. Plasmas* **22** 052304
[23] Li C-F 2003 *Geophys. J. Int.* **153** 201–12
[24] Johnson J C, Merlino R L and D'Angelo N 1989 *J. Appl. Phys.* D **22** 1456
[25] Johnson J C, Merlino R L and D'Angelo N 1990 *J. Appl. Phys.* D **23** 682–5
[26] D'Angelo N 1967 *Phys. Fluids.* **10** 719